THE EFFECT OF MALONIC ACID AND SUCCINIC ACID ON THE CORROSION BEHAVIOR OF Mg-5Zn IN $(NH_4)_3PO_4$ AND NaF

Yudi Nugraha Thaha[1][*], Nono Darsono[1], Muhammad Satrio Utomo[1], Djusman Sajuti[1], Ika Kartika[1]

[1]Research Center for Metallurgy and Materials, Indonesian Institute of Sciences
PUSPIPTEK Building 470, Tangerang Selatan 15343, Indonesia

ABSTRACT

While having excellent biocompatibility and biodegradability properties, magnesium alloys have been widely known to exhibit low corrosion resistance, especially in an acidic environment. The partially protective layer of $Mg(OH)_2$ plays an important role in the corrosion behavior of magnesium, while a phosphate and fluoride conversion film enhances the corrosion resistance of magnesium alloy. The comparative study of electrochemical corrosion behaviour of Mg-5Zn with different media was performed in 1% $(NH_4)_3PO_4$ and 1% NaF. The effect of malonic and succinic acid on the corrosion behaviour of Mg-5Zn was also analyzed. The back scattering electron mode of scanning electron microscopy was used to characterize the microstructure of Mg-5Zn alloys. Electrochemical impedance spectroscopy (EIS) and the potentiodynamic polarization curve were employed to study the electrochemical corrosion behaviour of Mg-5Zn. It was found that the presence of malonic and succinic acid decreases film resistance and enhances the electron transfer of Mg-5Zn in 1% $(NH_4)_3PO_4$ and 1% NaF. A higher Mg-5Zn dissolution rate was observed in a binary mixture of 1% malonic acid and 1% succinic acid with 1% $(NH_4)_3PO_4$ and 1% NaF in comparison with Mg-5Zn in 1% $(NH_4)_3PO_4$ and 1% NaF.

Keywords: Corrosion; Electrochemical impedance spectroscopy; Mg-5Zn; Potentiodynamic polarization

1. INTRODUCTION

Due to high stiffness and lightness to weight ratio and biocompatibility, magnesium and its alloys have received considerable attention in relation to biodegradable metallic implants (Virtanen, 2011). In energy storage applications, magnesium-based alloys and magnesium-based MgH_2 composites are potentially applied to hydrogen storage materials (Zulkarnain et al., 2016). Magnesium can be used to modify the hydrogen physisorption of SWCNTs (Supriyadi et al., 2016). Magnesium possesses low electrochemical potential in a galvanic series, which makes magnesium and its alloys highly reactive with a low corrosion resistance (Song & Atrens, 1999). The corrosion resistance of magnesium depends on the microstructure, grain boundary, phase distribution, and actual physiological environment (Pardo et al., 2008; Zhao et al., 2008; Nayak et al., 2016). The pH value of physiological fluid has a considerable effect on the corrosion rate of magnesium. Mg tends to corrode faster in acidic environment or pH with a neutral value to form Mg^{+2} (Song & Atrens, 1999). In an alkaline solution of pH 11, $Mg(OH)_2$ film is produced. A decrease in the corrosion rate of magnesium, Mg tends to corrode faster in acidic environment

or pH with a neutral value to form Mg^{+2} (Song & Atrens, 1999). In an alkaline solution of pH 11, $Mg(OH)_2$ film is produced. A decrease in the pH solution and the presence of chloride ion destabilize $Mg(OH)_2$ film (Song & Atrens, 1999). Recent works related to the electrochemical corrosion process of the ultrahigh purity of Mg-5Zn and the corrosion mechanism in magnesium alloys have been published (Song et al., 2012; Shi et al., 2015).

It was reported that phosphate and fluoride conversion film enhances the corrosion resistance of magnesium alloy (Chong & Shih, 2003; Chiu et al., 2007). The partially protective layer of $Mg(OH)_2$ plays an important role in the corrosion behavior of magnesium. A thin hydroxide layer on the magnesium surface is formed when magnesium and its alloys are exposed to water (Song & Atrens, 1999).

Interfacial kinetic studies of the metal release between magnesium alloys and their physiological environment are important to control the corrosion process in bio-electrochemical applications of magnesium alloy. In the human body, succinic acid is produced in mitochondria via the tricarboxylic acid cycle. Malonic acid functions as a competitive inhibitor of succisinate dehidrogenase in the respiratory electron transport chain. Succinic acid and malonic acid are important parts of the respiratory chain and Krebs cycle. Succinic and malonic acid play important roles in ATP production in the mitochondria (Chong & Shih, 2003; Akram, 2014). In cells, succinate can be released from the mitochondrial matrix to the cytoplasm through plasma membrane transporters. For damaged membrane cells and cell death, succinate can be released from the cytoplasm to the outer layer of the cell and can decrease the local pH of the cell membrane and the solution interface. Under pathophysiological conditions, succinate has been observed in the area of inflammation (Connors et al., 2018).

Mg-5Zn corrosion simulation in $(NH_4)_3PO_4$ and NaF 1% with the presence of malonic acid and succinic acid as a biochemical interference is not reported in any previous literature study. In this article, the comparative study of the electrochemical corrosion behavior of Mg-5Zn in $(NH_4)_3PO_4$ and NaF 1% and the effects of malonic acid and succinic acid on the corrosion behavior of Mg-5Zn in $(NH_4)_3PO_4$ and NaF are reported.

2.   METHODS

2.1. Materials
Magnesium (Mg) powder (99.9%) and zinc (Zn) powder (99.9%) were purchased from Merck and used as received without any further purification. Mg-5Zn was produced by powder metallurgy. The magnesium and zinc powder were mixed by a shaker mill and uniaxially pressed at 300 MPa to form green cylinder compacts of a diameter of 1 cm and a height of 5 mm at standard room temperature and pressure (25℃, 1 atm). The samples were then sintered in a tube furnace in an argon atmosphere at 650℃ for 2 h and cooled to room temperature in an inert atmosphere using argon gas.

2.2. Liquid Solution
Succinic acid, malonic acid, $(NH_4)_3PO_4$, and NaF were purchased from Merck without any further purification. For electrochemical measurements, a stock solution of 1% succinic acid, 1% malonic acid, 1% $(NH_4)_3PO_4$, and 1% NaF were used. All electrochemical experiments were performed at pH = 7, which resembles human physiological pH.

2.3. Characterization
The electrochemical measurement was employed on a Gamry G750 electrochemical working station. A potensiodynamic polarization curve measurement was performed in a glass cell with Mg-5Zn alloy as the working electrode. The counter electrode was a platinum wire, and an Ag/AgCl was used as the reference electrode. The electrochemical impedance spectra (EIS) were

measured at room temperature in the frequency range from 0.01 Hz to 100 kHz and an amplitude of 10 mV referring to Eoc. E-chem Analyst was used to analyze potensiodynamic and EIS data.

3.   RESULTS AND DISCUSSION

After the time parameters of the maskless photolithography process were found, the process was applied to PCB routing.

3.1.   Model and Real Profile Comparison

The size of the laptop model and the PCB profile required comparison to ensure the resulting profile. Square models of 10 mm to 100 mm were created on the laptop using a box colored light blue on a black background. The maskless photolithography process was then performed using previously established parameters (see sections 2.1 to 2.7): exposure of four minutes, development of three minutes, etching for two minutes, and removal for one minute.
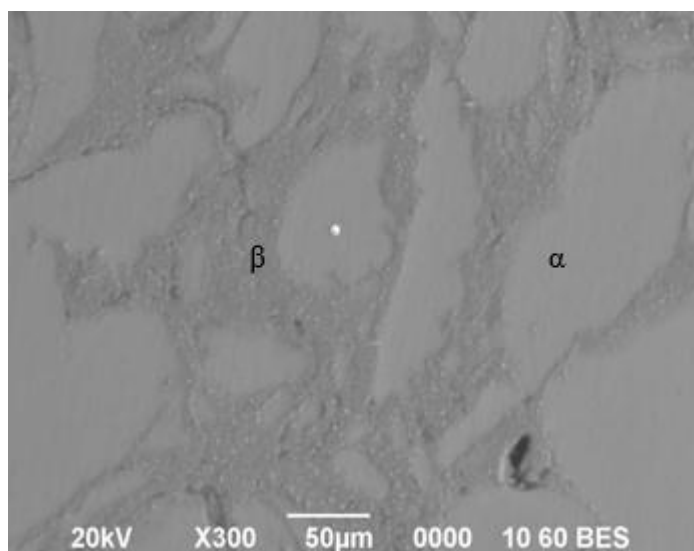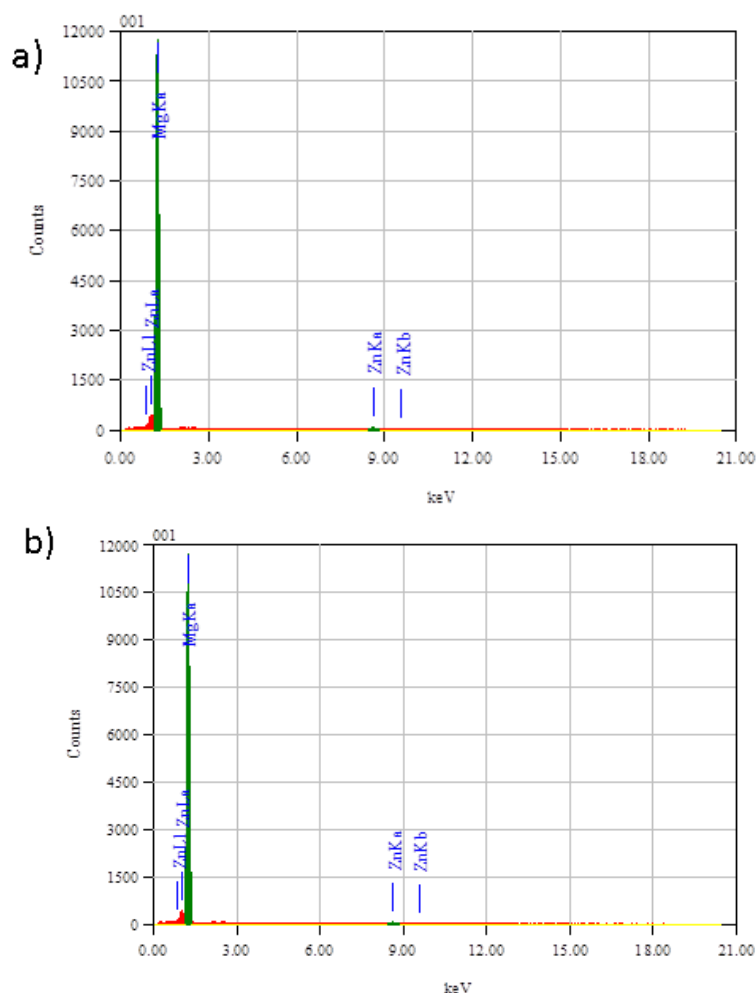

Figure 1 Image of scanning electron microscopy by the back scattering mode of Mg-5Zn shows the β phase in the α matrix

3.2.   Electrochemical Impedance Spectroscopy

Electrochemical impedance spectroscopy is widely used when studying the surface corrosion behavior of light metal alloys, such as aluminum alloys (Vika et al., 2015) and magnesium alloys (Santiago et al., 2018). In this present work, electrochemical impedance spectroscopy (EIS) characterization was performed for an open circuit potential on Mg-5Zn in 1% NaF, 1% (NH$_4$)$_3$PO$_4$, and a binary mixture of malonic acid and succinic acid with 1% NaF and 1% (NH$_4$)$_3$PO$_4$, as shown in Figures 3a–3f. The Nyquist plot of impedance spectra is displayed as the sum of real and imaginary impedance. The impedance spectra were analyzed using Echem Analyst. The quantification of electrochemical impedance spectroscopy parameters was performed using the simplex method (Nelder & Mead, 1965).

Charge transfer resistance R_{ct} and film resistance R_f were analyzed using an equivalent circuit, as shown in Figures 3a and 3b. In an equivalent circuit, R_{ct} is charge transfer resistance, R_f is film resistance, and CPE is constant phase elements. EIS spectra represent the electrochemical process on the electrode surface. The charge transfer resistance and film resistance obtained from an equivalent circuit numerical simulation of EIS spectra are presented in Table 1.

Figure 2 Energy dispersive X-ray spectroscopy of Mg-5Zn: (a) β phase composition; and (b) α phase composition

The EIS spectra of Mg-5Zn in 1% $(NH_4)_3PO_4$, 1% $(NH_4)_3PO_4$ with malonic acid, and 1% $(NH_4)_3PO_4$ with succinic acid were characterized with a depressed semicircle at high and medium frequencies with inductance at a low frequency. Inductance at a low frequency represents the characteristics of adsorbed species and the relaxation process on the $Mg(OH)_2$ surface (Pebere et al., 1990). The equivalent circuit model in Figure 3a was applied to estimate the charge transfer resistance and film resistance of Mg-5Zn in 1% $(NH_4)_3PO_4$, 1% $(NH_4)_3PO_4$ with malonic acid, and 1% $(NH_4)_3PO_4$ with succinic acid.

Mg-5Zn in 1% $(NH_4)_3PO_4$ exhibited a lower transfer resistance in comparison with Mg-5Zn in 1% NaF. Variations in charge transfer resistance indicate variations in the electrochemical behavior of Mg-5Zn in different solutions. Mg-5Zn in 1% $(NH_4)_3PO_4$ with succinic acid and 1% $(NH_4)_3PO_4$ with malonic acid exhibited the lowest charge transfer resistance in comparison with Mg-5Zn in 1% $(NH_4)_3PO_4$. Similar experimental trends were observed in EIS measurements of Mg-5Zn in 1% NaF. The equivalent circuit model shown in Figure 3b was applied to characterize the charge transfer resistance and film resistance Mg-5Zn in 1% NaF, 1% NaF with malonic acid, and 1% NaF with succinic acid.
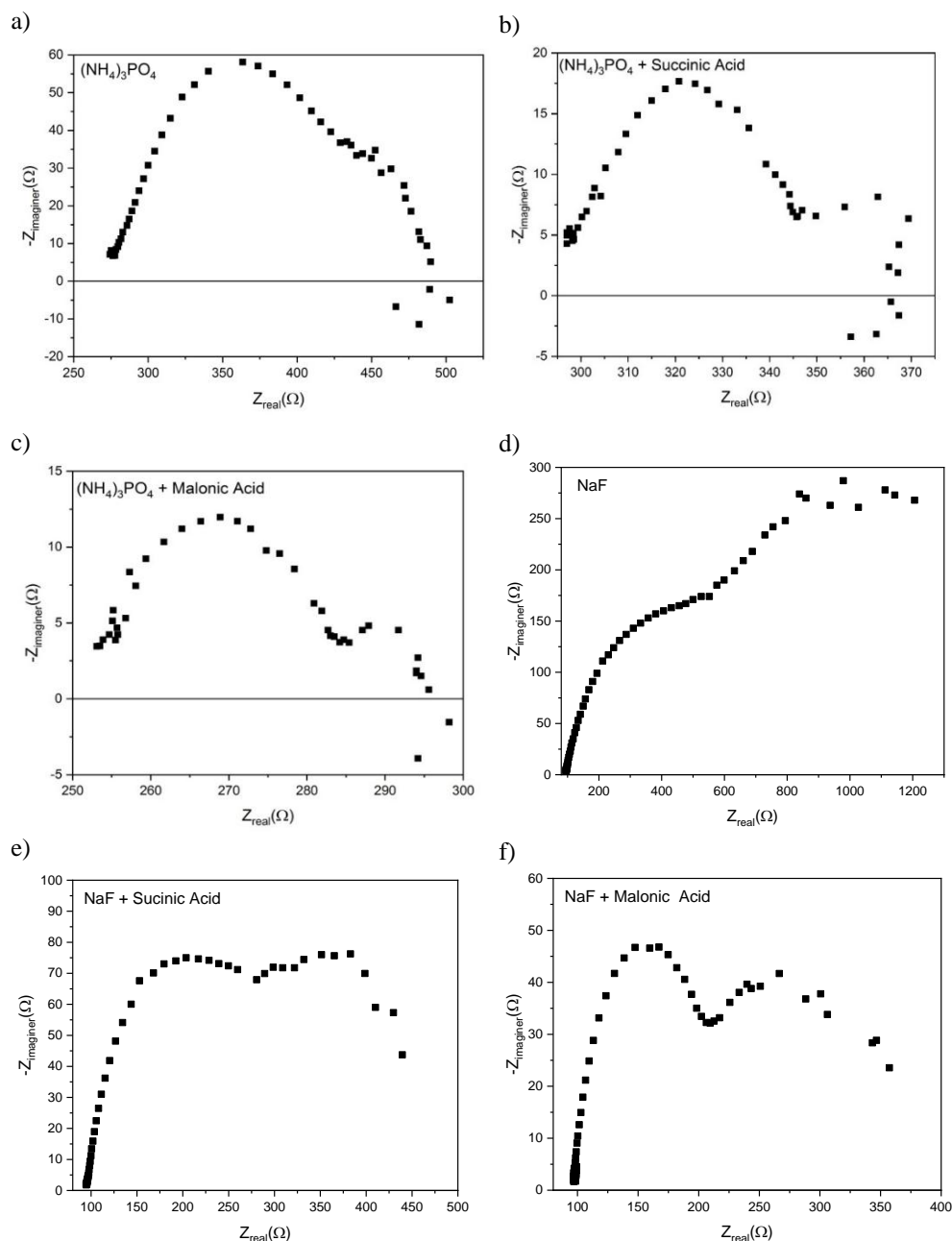
Figure 3 Representative EIS spectra for Mg-5Zn recorded in: (a) (NH$_4$)$_3$PO$_4$; (b) (NH$_4$)$_3$PO$_4$ + Succinic Acid; (c) (NH$_4$)$_3$PO$_4$ + Malonic Acid; (d) NaF; (e) NaF + Succinic Acid; and (f) NaF + Malonic Acid

The presence of malonic acid and succinic acid lead to a decrease of resistance against electron transfer. The lower value of charge transfer resistance of Mg-5Zn in 1% (NH$_4$)$_3$PO$_4$ and 1% NaF with 1% succinic acid and 1% malonic acid can be explained by an acid base reaction between succinic acid and malonic acid, and the Mg(OH)$_2$ film surface on the Mg-5Zn alloy acid reduces the Mg(OH)$_2$ layer's film thickness. The decrease in the Mg(OH)$_2$ layer film thickness increases electron transfer between Mg-5Zn and the solution. The reduction in the Mg(OH)$_2$ layer film thickness is supported by the experimental results, demonstrating a decrease in the R$_f$ value of Mg-5Zn in 1% (NH$_4$)$_3$PO$_4$ and 1% NaF due to the presence of malonic acid and succinic acid.
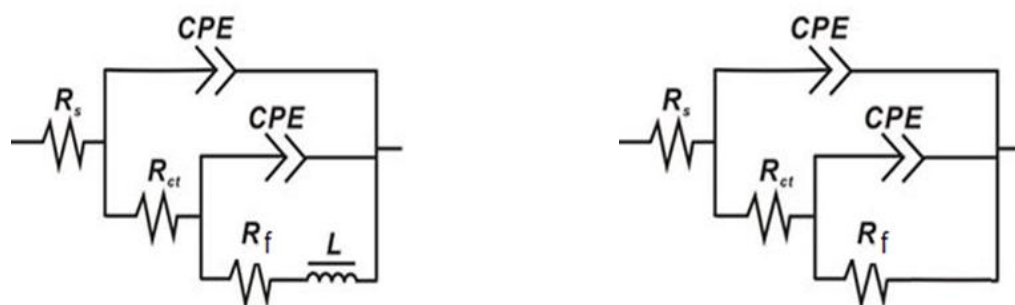
Figure 4 Equivalent circuit used to model the impedance spectra measured on the Mg-5Zn alloys: (a) in $(NH_4)_3PO_4$, $(NH_4)_3PO_4$ + Succinic Acid, and $(NH_4)_3PO_4$ + Malonic Acid; (b) in NaF, NaF + Succinic Acid and NaF + Malonic Acid

Table 1 EIS fitting parameters of Mg-5Zn in various media

Material	Solution	R_{ct}/Ω	R_f/Ω
Mg-5Zn	$(NH_4)_3PO_4$	187.50	24.33
Mg-5Zn	$(NH_4)_3PO_4$ + 1% Malonic acid	35.45	18.89
Mg-5Zn	$(NH_4)_3PO_4$ + 1% succinic acid	56.10	10.82
Mg-5Zn	NaF	493.50	753
Mg-5Zn	NaF + 1% malonic acid	111.10	42.28
Mg-5Zn	NaF + 1% succinic acid	198	184.90

Ab initio molecular orbital studies show that magnesium ion interacts with malonate in a chelation bidentate orientation (Deerfield et al., 1991). Magnesium succinate exhibits high solubility in water. The formation of a magnesium-succinate complex is strongly affected by temperature and ion strength in the solution (de Robertis et al., 1984).

3.3. Potentiodynamic polarization

The corrosion reaction kinetics of magnesium and magnesium alloy are determined by the anodic dissolution of magnesium and the cathodic water decomposition reaction into hydrogen and hydroxide cations (Greenblatt, 1958). For magnesium, the rate of hydrogen evolution rises gradually when applying polarization potential, and current density becomes more positive in the anodic region (Zhang, 2018). For a thermodynamic comparison (relative to a standard hydrogen electrode [NHE]), the corrosion potential of magnesium with water (Mg+ $2H_2O \rightarrow 2H_2 + O_2 + 2OH^-$, $E° = 0.177$ V) is lower than water oxidation ($2H_2O \rightarrow 4H^+ + 4e^- + O_2$ $E° = 1.23$ V). These values indicate that in a certain range, magnesium corrosion can be characterized by potentiodynamic polarization without oxygen interference from water splitting.

The potentiodynamic polarization characterization produced snapshots of the kinetic corrosion process at the time it was measured. Potensiodynamic polarization measurements were applied to confirm the electrochemical impedance measurements. Figure 4 displays the potensiodynamic polarization curve of Mg-5Zn in 1% $(NH_4)_3PO_4$, 1% NaF, a binary mixture of 1% $(NH_4)_3PO_4$ with 1% succinic acid and with 1% malonic acid, and a binary mixture of 1% NaF with 1% succinic acid and with 1% malonic acid.

The fitting parameter results of the potentiodynamic polarization curve, including corrosion current density and corrosion potential, are presented in Table 2. The potentiodynamic polarization curve exhibited a Tafel behavior characteristic in the anodic and cathodic branches. A passive region was not clearly observed in the potentiodynamic polarization curve.
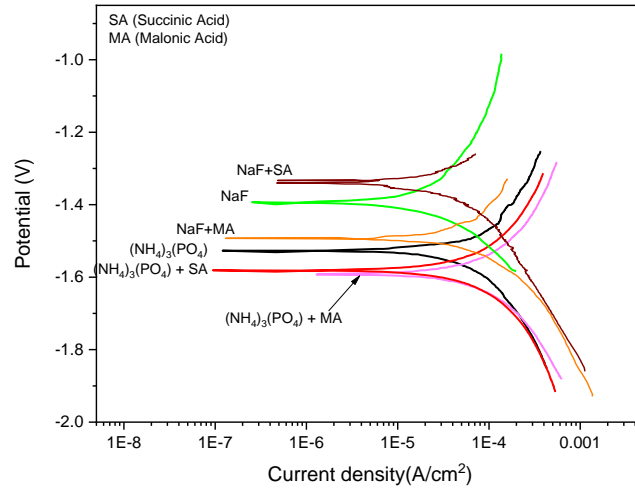
Figure 5 Potentiodynamic polarization curve for Mg-5Zn in Mg-5Zn in 1% (NH$_4$)$_3$PO$_4$, 1% NaF, a binary mixture of 1% (NH$_4$)$_3$PO$_4$ with 1% succinic acid and with 1% malonic acid, and a binary mixture of 1% NaF with 1% succinic acid and with 1% malonic acid.

The corrosion potential of Mg-5Zn in 1% NaF is higher than the corrosion potential of Mg-5Zn in 1% (NH$_4$)$_3$PO$_4$. This result indicates that Mg-5Zn in 1% NaF is nobler than Mg-5Zn in 1% (NH$_4$)$_3$PO$_4$. The presence of succinic acid and malonic acid in (NH$_4$)$_3$PO$_4$ decreases the corrosion potential of Mg-5Zn.

Table 2 Potentiodynamic fitting parameters of Mg-5Zn in various media

Material	Solution	E_{corr} (V)	I_{coor} (A/cm²) 10^{-6}	Corrosion Rates (mmpy)
Mg-5Zn	(NH$_4$)$_3$(PO$_4$)	-1.527	81.37	1.795
Mg-5Zn	1% (NH$_4$)$_3$(PO$_4$) 1% Malonic Acid	-1.593	141.1	3.114
Mg-5Zn	(NH$_4$)$_3$(PO$_4$) 1% Succinic Acid	-1.581	153.2	3.379
Mg-5Zn	NaF	-1.393	28.40	0.627
Mg-5Zn	NaF +1% Malonic Acid	-1.494	154.4	3.406
Mg-5Zn	NaF +1% Succinic Acid	-1.340	63.84	1.408

The corrosion current density of Mg-5Zn in (NH$_4$)$_3$PO$_4$ with succinic acid and malonic acid is higher than that of Mg-5Zn in (NH$_4$)$_3$PO$_4$, demonstrating the effect of succinic acid and malonic acid on the kinetic of corrosion rate of Mg-5Zn. Mg-5Zn in 1% (NH$_4$)$_3$PO$_4$ exhibited a higher corrosion resistance in comparison with that of Mg-5Zn in Mg-5Zn in (NH$_4$)$_3$PO$_4$ with succinic acid and malonic acid. A similar trend of electrochemical corrosion behavior was observed in Mg-5Zn in 1% NaF.

4. CONCLUSION

In this work, the electrochemical corrosion behavior of powder metallurgy Mg-5Zn was examined in a binary mixture of 1% (NH$_4$)$_3$PO$_4$ with 1% succinic acid and with 1% malonic acid and a binary mixture of 1% NaF with 1% succinic acid and with 1% malonic acid. The back scattering electron mode of scanning electron microscopy was used to characterize the microstructure of Mg-5Zn alloys. Electrochemical impedance spectroscopy was employed to investigate the electrochemical process on the Mg-5Zn alloy surface. Potentiodynamic polarization was used to characterize the kinetics of the corrosion of Mg-5Zn. It was observed that the presence of 1% succinic acid and 1% malonic acid enhanced the corrosion process of

Mg-5Zn in 1% $(NH_4)_3PO_4$ and 1% NaF. The acid-base reaction between $Mg(OH)_2$ with succinic acid and malonic acid on the Mg-5Zn surface promoted the degradation rate of Mg-5Zn alloys.

5. ACKNOWLEDGEMENT

6. REFERENCES

Akram, M., 2014. Citric Acid Cycle and Role of Its Intermediates in Metabolism. *Cell Biochemistry and Biophysics*, Volume 68(3), pp. 475–478

Chiu, K.Y., Wong, M.H., Cheng, F.T., Man, H.C., 2007. Characterization and Corrosion Studies of Fluoride Conversion Coating on Degradable Mg Implants. *Surface and Coatings Technology*, Volume 202(3), pp. 590–598

Chong, K.Z., Shih, T.S., 2003. Conversion-coating Treatment for Magnesium Alloys by a Permanganate-phosphate Solution. *Materials Chemistry and Physics*, Volume 80(1), pp. 191–200

Connors, J., Dawe, N., Limbergen, J.V., 2018. The Role of Succinate in the Regulation of Intestinal Inflammation. *Nutrients*, Volume 11(1), pp. 1–12

Deerfield, D.W., Fox, D.J., Head-Gordon, M., Hiskey, R.G., Pedersen, L.G., 1991. Interaction of Calcium and Magnesium Ions with Malonate and the Role of the Waters of Hydration: A Quantum Mechanical Study. *Journal of the American Chemical Society*, Volume 113(6), pp. 1892–1899

Greenblatt, J.H., 1958. Note on the Rate of Evolution of Hydrogen at a Magnesium Anode. *Canadian Journal of Chemistry,* Volume 36(8), pp. 1138–1140

Nayak, S., Bhushan, B., Jayaganthan, R., Gopinath, P., Agarwal, R.D., Lahiri, D., 2016. Strengthening of Mg Based Alloy through Grain Refinement for Orthopaedic Application. *Journal of Mechanical Behavior of Biomedical Material*, Volume 59, pp. 57–70

Nelder, J.A., Mead, R., 1965. A Simplex Method for Function Minimization. *The Computer Journal*, Volume 7(4), pp. 308–313

Pardo, A., Merino, M.C., Coy, A.E., Viejo, F., Arrabal, R., Feliu, S., 2008. Influence of Microstructure and Composition on the Corrosion Behaviour of Mg/Al Alloys in Chloride Media. *Electrochimica Acta*, Volume 53(27), pp. 7890–7902

Pebere, N., Riera, C., Dabosi, F., 1990. Investigation of Magnesium Corrosion in Aerated Sodium Sulfate Solution by Electrochemical Impedance Spectroscopy. *Electrochimica Acta*, Volume 35(2), pp. 555–561

de Robertis, A.D., de Stefano, C., Scarcella, R., Rigano, C., 1984. Thermodynamics of Formation of Magnesium(II), Calcium(II), Strontium(II) and Barium(II)-Succinate Complexes in Aqueous Solution. *Thermochimica Acta*, Volume 80(2), pp. 197–208

Santiago, F., Federico, R. Garcia, G., Violeta, B., Juan, C.G., Sebastian, F.B, 2018. *A Critical Review of the Application of Electrochemical Technique for Studying Corrosion of Mg and Mg Alloys: Opportunities and Challenges,*.Intechopen, London, UK, pp. 5–28

Shi, Z., Hofstetter, J., Cao, F., Uggowitzer, P.J., Dargusch, M.S., Atrens, A., 2015. Corrosion and Stress Corrosion Cracking of Ultra-high-purity Mg5Zn. *Corrosion Science*, Volume 93, pp. 330–335

Song, G.L., Atrens, A., 1999. Corrosion Mechanisms of Magnesium Alloys. *Advanced Engineering Materials*, Volume 1(1), pp. 11–33

Song, Y., Han, E.H., Shan, D., Yim, C.D., You, B.S., 2012. The Role of Second Phases in the Corrosion Behavior of Mg-5Zn Alloy. *Corrosion Science*, Volume 60, pp. 238–245

Supriyadi, S., Nasruddin, N., Engkos, A., Kosasih, Budhy, K., Zulkarnain, I. A., 2016. Improving Hydrogen Physisorption Energy using SWCNTS through Structure Optimization and Metal Doping Substitution. *International Journal of Technology*, Volume 7(8), pp. 1455–1463

Vika, R., Badrul. M., Johny, W.S., Bambang, S., 2015. Corrosion Resistance Enhancement of an Anodic Layer on an Aluminum Matrix Composite by Cerium Sealing. *International Journal of Technology*, Volume 6(7), pp. 1191–1197

Virtanen, S., 2011. Biodegradable Mg and Mg Alloys: Corrosion and Biocompatibility. *Materials Science and Engineering B*, Volume 176(20), pp. 1600–1608

Zhao, M.C., Liu, M., Song, G., Atrens, A., 2008. Influence of the β-phase Morphology on the Corrosion of the Mg Alloy AZ91. *Corrosion Science*, Volume 50(7), pp. 1939–1953

Zhang, W., Qijun, Liu., Yingqi, C., Guojiang, W., 2018. Anodic Dissolution Dictates the Negative Difference Effect of Magnesium Corrosion More in a Chemical Pathway. *Material Letters*, Volume 232, pp. 54–57

Zulkarnain , J., Adi, R., Farid, M., Mustanir, M., 2016. Desorption Temperature Characteristic of Mg-based Hydrides Catalyzed by Nano-SiO_2 Prepared by High Energy Ball Milling. *International Journal of Technology*, Volume 7(8), pp. 1301–1306